Leak Rate Performance of Silicone Elastomer O-Rings Contaminated with JSC-1A Lunar Regolith Simulant

H.A. Oravec and C.C. Daniels

The University of Akron, College of Engineering, Akron, OH; email: horavec@uakron.edu and cdaniels@uakron.edu

ABSTRACT

Contamination of spacecraft components with planetary and foreign object debris is a growing concern. Face seals separating the spacecraft cabin from the debris filled environment are particularly susceptible; if the seal becomes contaminated there is potential for decreased performance, mission failure, or catastrophe. In this study, silicone elastomer O-rings were contaminated with JSC-1A lunar regolith and their leak rate performance was evaluated. The leak rate values of contaminated O-rings at four levels of seal compression were compared to those of as-received, uncontaminated, O-rings. The results showed a drastic increase in leak rate after contamination. JSC-1A contaminated O-rings lead to immeasurably high leak rate values for all levels of compression except complete closure. Additionally, a mechanical method of simulant removal was examined. In general, this method returned the leak rate to as-received values.

NOMENCLATURE

a_0, a_1	=	regression coefficients	ϕ	=	precision error
β	=	bias error	R	=	specific gas constant
i, k	=	indices	ρ	=	correlation coefficient
m	=	mass	T	=	temperature
$\dot{m}$	=	mass leak rate	t	=	time
N	=	number of samples	$U_{\dot{m}}$	=	leak rate uncertainty
p	=	absolute pressure	V	=	volume

INTRODUCTION

Contamination of spacecraft components with foreign object debris (FOD) can be detrimental to the safety and success of space missions. Aerospace face seals, in particular, are designed to separate a sustainable environment from the uninhabitable vacuum of space. If the face seal becomes contaminated with FOD there is potential for decreased performance, mission failure, or even loss of human life.

FOD is a foreign body, not associated with the system or its components, that has potential to cause damage. In terms of spacecraft components, it can result from

poorly kept ground facilities, orbital debris in the form of meteoroids and discarded space equipment (NASA, 1995), and even the planetary environment such as lunar dust (Gaier, 2005). In 2013, the National Aeronautics and Space Administration (NASA) tracked over 500,000 pieces of both naturally occurring and manufactured space debris (NASA, 2013). With millions of additional FOD that are too small to trace, the potential danger of contamination becomes a realistic threat. In fact, during the Apollo missions, planetary FOD in the form of lunar dust caused a significant decrease in the leak rate performance of the face seals on extravehicular mobility unit spacesuits (Gaier, 2005).

One of the most prominent face seals in spacecraft sealing applications is the main docking interface seal which is necessary for vehicle-vehicle and vehicle-structure mating. Historically, docking seals have been made from silicone elastomers (Finkbeiner, Dunlap, Steinetz, & Daniels, 2008). Silicone elastomers are preferred for space seals, versus their metal counterparts, because of their wide range of operating temperatures and reusability (Parker Hannifin Corporation, 2001). Additionally, silicone elastomers meet essential programmatic and performance requirements such as low-outgassing standards (ASTM International, 2003; NASA, 2007), operation in the harsh space environment (Garafolo, Bastrzyk, & Daniels, 2010) including vacuum (Carrell & Blair, 1964), compression force requirements (Bastrzyk & Daniels, 2010; Oravec, Panickar, Wasowski, & Daniels, 2011), and leak rate requirements (Daniels & Garafolo, 2010). However, few studies have considered the contamination of silicone elastomer seals with FOD (Garafolo & Daniels, 2011).

For future exploration missions to low-earth orbit and beyond it is important to understand the impact of FOD on docking seals. Whether manmade or planetary, FOD may significantly impact the performance of these seals causing loss of cabin pressure or worse. Given the lack of experimental data on FOD contaminated docking seals, as previously mentioned, the objective of this study was to investigate the leak rate performance of silicone elastomer O-rings contaminated with JSC-1A lunar regolith simulant representative of planetary FOD. A series of leak rate tests was run on O-rings contaminated with JSC-1A at four increasing levels of seal compression. In addition, a mechanical method of simulant removal was investigated. The results of these tests were presented herein.

DESCRIPTION OF EXPERIMENTS

A series of experiments was run to quantify and characterize the leak rate performance of silicone elastomer O-rings contaminated with JSC-1A lunar regolith simulant. A description of the methodology, test articles, apparatus, FOD contaminant, and experimental procedure were described in the following paragraphs.

Test Methodology. The leak rate performance was characterized through the pressure decay method with mass point leak rate analysis (Daniels & Garafolo, 2010; Garafolo & Daniels, 2010; Garafolo & Daniels, 2014; Moore, Jackson, & Sherlock, 1998). This test method had advantages when compared to other methods as it could be used to quantify a wide range of leak rates without knowing the approximate leak rate *a priori*. The method required a test apparatus with a hermetically sealed control

volume of gas; all leakage was attributed to the test article of interest. The volume size was quantified in advance using *Boyle's Law* (Garafolo, 2010). Approximately two atmospheres pressure of dry air was supplied to the control volume and allowed to decay as the gas flowed around and permeated through the test article and into ambient atmosphere. The gas pressure and temperature were recorded over time. The *Ideal Gas Law* was assumed and the mass of gas within the system was calculated using the following equation.

$$m = \frac{pV}{RT} \tag{1}$$

For every time-step, the mass of the gas was calculated yielding a mass-time population (t_i, m_i). Assuming a constant leak rate; a linear least-squares regression was computed for the mass-time population, centered about the differential pressure of 14.7 psid, which resulted in Equation 2,

$$m(t) = a_1 t + a_0 \tag{2}$$

where the first-order regression coefficient a_1 was the slope of the best fit line and represented the leak rate of the test article. A typical mass regression plot was shown in Figure 1.

The uncertainty of the leak rate was calculated using the generalized Equation 3 (Daniels & Garafolo, 2010; Garafolo & Daniels, 2010; Garafolo & Daniels, 2014). The development of the uncertainty parameter included the effects of bias and precision for each measurement, but for brevity was not shown herein. For more detailed information refer to Daniels & Garafolo, 2010; Garafolo & Daniels, 2010; and Garafolo & Daniels, 2014.

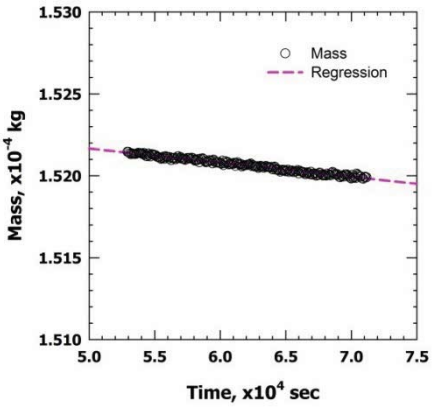

Figure 1. Typical mass regression plot.

$$\begin{aligned} U_{\dot{m}}^2 = & \sum_{i=1}^{N} \left(\frac{\partial \dot{m}}{\partial m_i}\right)^2 \beta_{m_i}^2 + \sum_{i=1}^{N} \left(\frac{\partial \dot{m}}{\partial t_i}\right)^2 \beta_{t_i}^2 + \sum_{i=1}^{N} \left(\frac{\partial \dot{m}}{\partial m_i}\right)^2 \phi_{m_i}^2 + \sum_{i=1}^{N} \left(\frac{\partial \dot{m}}{\partial t_i}\right)^2 \phi_{t_i}^2 \\ & + 2 \sum_{i=1}^{N-1} \sum_{k=i+1}^{N} \left(\frac{\partial \dot{m}}{\partial m_i}\right)\left(\frac{\partial \dot{m}}{\partial m_k}\right) \rho_{m_i m_k} \beta_{m_i} \beta_{m_k} \\ & + 2 \sum_{i=1}^{N-1} \sum_{k=i+1}^{N} \left(\frac{\partial \dot{m}}{\partial t_i}\right)\left(\frac{\partial \dot{m}}{\partial t_k}\right) \rho_{t_i t_k} \beta_{t_i} \beta_{t_k} \\ & + 2 \sum_{i=1}^{N-1} \sum_{k=i+1}^{N} \left(\frac{\partial \dot{m}}{\partial t_i}\right)\left(\frac{\partial \dot{m}}{\partial m_k}\right) \rho_{t_i m_k} \beta_{t_i} \beta_{m_k} \end{aligned} \tag{3}$$

Test Articles. The test articles were standard AS568A size 2-309 O-rings manufactured from S0383-70 silicone elastomer compound by the Parker Hannifin Corporation (Parker Hannifin Corporation, 2001). The nominal dimensions of the specimens were shown in Table 1. A total of 24 2-309 O-ring test articles were utilized in this study. Those O-rings in an as-received from the manufacturer condition were referred to herein as as-received test articles. Those O-rings coated with JSC-1A were referred to herein as contaminated test articles.

Table 1. Nominal dimensions of the 2-309 O-ring test articles.

Inner Diameter, mm	Width, mm
10.46 ± 0.13	5.33 ± 0.13

Test Apparatus. The test apparatus consisted of two stainless steel platens, pressure and temperature transducers, and near hermetic plumbing; all having a leak rate below 10^{-9} atm·cc/sec as verified by a helium leak detector. The stainless steel platens had a surface finish of 0.41 μm or better. The lower platen was flat and simulated a seal-to-metal docking interface. The upper platen was designed with a groove to receive the test article and allowed for maximum nominal compression equal to 25% of the total O-ring height.

The control volume was created by clamping the test article between the two platens, Figure 2. Since each test article was leak tested at four levels of compression (refer to Test Procedure), a total of four different volumes were quantified for use in Equation 1. The volume for each compression level was determined using an average of 248 applications of *Boyle's Law* (i.e., $P_1V_1 = P_2V_2$). The size of the volume was listed in Table 2 for each of the four levels of compression.

The pressure in the inner control volume was monitored by two pressure transducers with a full-scale range of 35 psia and corresponding accuracy better than ± 0.75%. The two pressure readings were averaged at each time step and the average values were used in the data analysis. The downstream barometric pressure was monitored using a single pressure transducer with similar accuracy.

The temperature was monitored using a Class A accuracy resistance temperature detector (RTD). A foam cover insulated the apparatus from the laboratory environment to minimize fluctuation in temperature. All tests were conducted at room temperature, approximately 23°C.

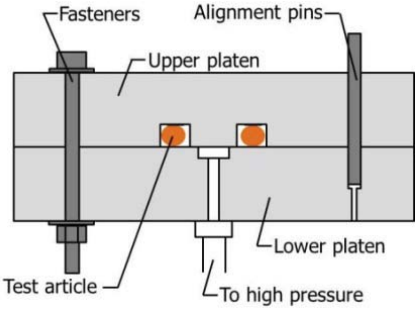

Figure 2. Cross-section of leak rate test apparatus.

Table 2. Control volume at four levels of compression.

Compression Level (%)	Volume (mL)
25	64.32
50	64.23
75	64.17
100	64.03

FOD Contaminant. To simulate contamination with planetary FOD, the widely available lunar regolith simulant JSC-1A was applied to a subset of test articles. The simulant was produced by Orbital Technologies Corporation to approximate the bulk mare regolith and had grain sizes of 1 mm and below. In geotechnical terms, JSC-1A was defined as poorly-graded silty sand (Zeng, He, Oravec, Wilkinson, Agui, & Asnani, 2010). A micrograph image of JSC-1A was shown in Figure 3 for reference.

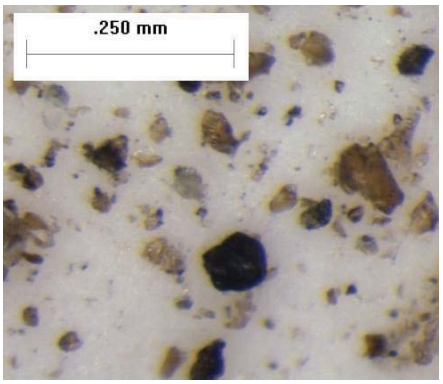

Figure 3. Micrograph image of JSC-1A at 10x magnification.

A subset of test articles was randomly selected to be leak rate tested after contamination with JSC-1A. The test surface of each O-ring was contaminated with JSC-1A by placing the O-rings, test side down, in a Petri dish containing an evenly spread layer of simulant. A 200 g weight was placed on each O-ring for a minimum of 30 seconds and then removed. The test articles were carefully removed from the simulant. Any loose particles were removed by tapping the side of each O-ring against the inner wall of the Petri dish. Each O-ring was then weighed to determine the amount of JSC-1A contamination. For the subset of test articles, the average amount of contamination, by weight, was 6.3 ± 1.0 mg.

The same test articles were also leak tested after attempting to mechanically remove the lunar simulant. The contaminated surface of each test article was dusted with an acid brush in a uniform circumferential pattern. The average weight of JSC-1A remaining after the brushing process was 2.2 ± 0.4 mg. These O-rings were referred to herein as cleaned test articles. Micrograph images of an as-received, contaminated, and cleaned test article were shown in Figure 4 for reference.

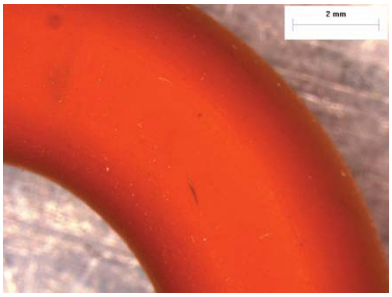

(a) As-received test article.

(b) Contaminated test article.

(c) Mechanically cleaned test article.

Figure 4. Typical micrograph images of 2-309 O-rings at 1.25x magnification.

Test Procedure. Using the aforementioned pressure decay method with mass point leak rate analysis, the leak rate of 24 2-309 O-rings was characterized at room temperature. All test articles were initially in an as-received from the manufacturer condition and had been cleaned with isopropyl alcohol. Of the 24 O-rings, a subset of 12 was leak rate tested in the as-received condition. The remaining 12 were tested after contamination with JSC-1A. The 12 test articles contaminated with JSC-1A were also leak tested after implementation of the mechanical method to remove the simulant from the test surface.

For each test condition, a total of four different compression levels were evaluated: 25, 50, 75, and 100% compression with respect to the nominal unconstrained O-ring height (i.e., when sitting uncompressed in the upper platen groove, the free height of the O-ring extending below the platen surface, Figure 5). For reference, the compression level based on unconstrained O-ring height was compared to the compression level based on the total O-ring height, Table 3. To achieve each level of compression, the platens were separated by placing metal shims equally spaced about the fixture bolts. For example, in the case of 25% compression, shims were placed between the platens such that the O-ring was compressed by 25% of its free height. In the case of 100% compression, no shims were required and the platens made metal-to-metal contact. Three replicate tests were performed for each test condition and compression level, Table 4.

Table 3. Unconstrained compression level versus total O-ring compression.

Unconstrained Compression Level (%)	Total O-ring Compression (%)
25	6
50	13
75	19
100	25

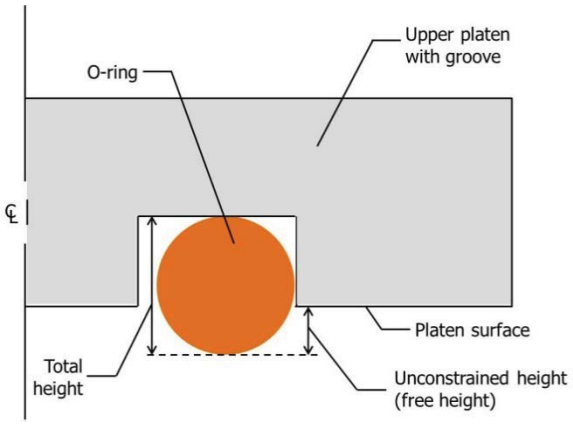

Figure 5. Cross-section of upper platen illustrating unconstrained (free) and total O-ring height.

For each experiment, the test article was placed in the groove of the upper platen such that the test surface (i.e., the contaminated surface of contaminated test articles) was facing outward. The lower platen was installed on the upper platen and bolted in place with three screws torqued to a uniform value. The internal control volume was evacuated and refilled with dry air three times to ensure that only dry air remained. The volume was then filled with dry air to a pressure of approximately two times atmospheric pressure. The test apparatus was enclosed in foam with no other means of temperature control. The mass of the control volume was allowed to

decay and the data reduction techniques were implemented for a pressure differential of 14.7 psid.

Table 4. Leak rate test matrix.

Test Condition	Compression Level (%)	Number of Replicates
As-received	25, 50, 75, 100	3
Contaminated	25, 50, 75, 100	3
Cleaned	25, 50, 75, 100	3

RESULTS

The results of the leak tests on as-received, contaminated, and mechanically cleaned 2-309 O-rings were summarized in Figure 6 with 95% confidence level in uncertainty. As-received test articles ranged in leak rate from 2.0×10^{-6} to 6.5×10^{-7} lb_m/day for 25% and 100% compression levels, respectively. For these test articles, a one way ANOVA test was implemented to compare the means of the four groups (i.e., compression levels). With 95% confidence, there was a statistically significant difference between the mean values of the groups. Thus, it could be stated that as the compression level increased, the leak rate of the as-received test articles decreased.

Contamination with JSC-1A severely impacted the leak rate of the test articles. In general, the JSC-1A contaminated O-rings had leak rate values that were too high to measure with the current system. Of the 12 tests on JSC-1A contaminated test articles only one leak rate was quantifiable. This leak rate corresponded to a single test article at 100% compression. Its value and corresponding measurement uncertainty were shown in Figure 6. This leak rate value was four orders of magnitude greater than the leak rates measured for the as-received test articles. However, because two of the three test articles within this group had leak rate values that were too high to quantify, the average leak rate value for contaminated test articles at 100% compression may have been even higher than that reported in Figure 6.

The mechanical action of the cleaning method produced a significant improvement in the leak rate of the test articles when compared with those that were not brushed clean. Although the test articles were not restored back to their pre-contamination state (some JSC-1A particles remained on the surface and may have become embedded during compression) the leak rates of the cleaned seals were several orders of magnitude lower than those that had not been cleaned, Figure 6. The cleaning method successfully restored the leak rate values of contaminated seals at 75% and 100% compression back to as-received values within the calculated level of uncertainty. Although the cleaned test articles at 25% and 50% compression appeared to have reduced leak rates in Figure 6, it should be noted that these values represented the average of only two replicate tests. The third replicate tests for the 25% and 50% compression levels had leak rate values that were too high to be measured with the current system. Thus, the average leak rate values may have been higher than those reported in Figure 6. Additionally, the mean leak rate values for cleaned test articles were compared and with 95% confidence, there was a statistically significant difference between the mean values of the four groups. Again, it could be

stated that as the compression level increased, the leak rate of the cleaned test articles decreased.

It should be noted that the cleaning method took place in laboratory conditions, not in a microgravity, vacuum-pressure environment. The humid air of the laboratory helped mitigate the electrostatic attraction between the simulant and the brush that would otherwise take place in a vacuum. The force of gravity in the laboratory also helped carry the debris away from the test article when removed from the surface. In a microgravity environment, removed debris may land back on the test surface.

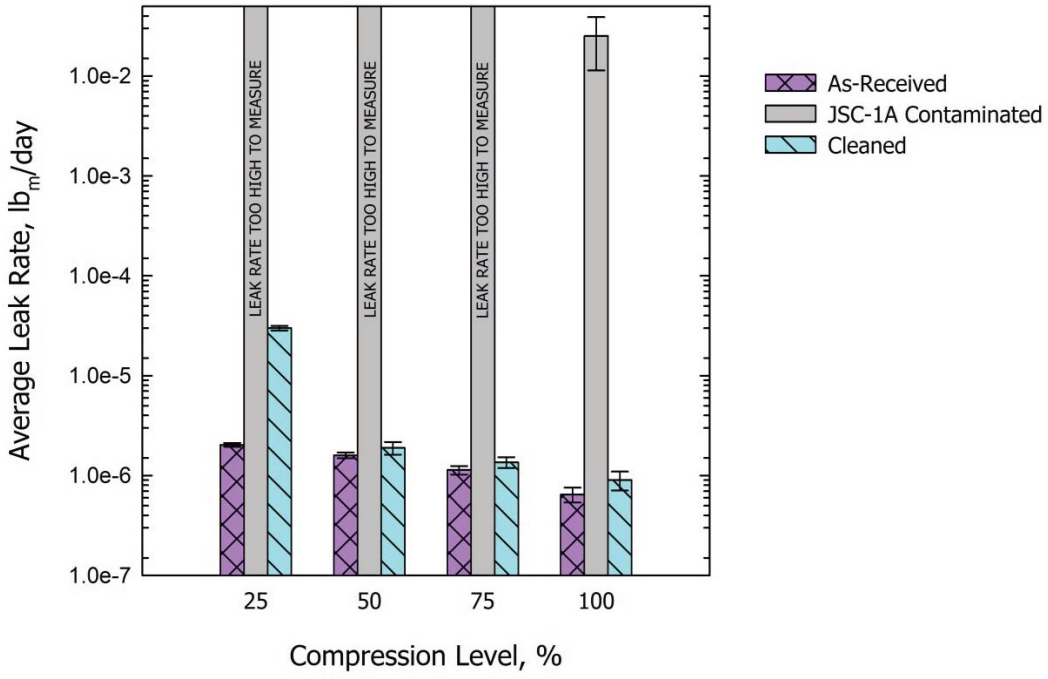

Figure 6. Average leak rate and corresponding uncertainty of as-received, contaminated, and cleaned 2-309 O-rings.

CONCLUSIONS

The safety and success of future space missions to low-Earth orbit and beyond depends on the ability of exposed face seals to operate when contaminated with FOD. With the amount of orbital debris on the rise and missions planned to planetary bodies with dusty environments, it is necessary to understand the functioning of face seals, including silicone elastomer docking seals, when contaminated with FOD. The results of this study showed that there is a definite need for a mitigation technique of FOD on elastomer seals.

The following conclusions were supported by the experimental investigation: (1) the leak rate decreased with increased compression level for as-received and cleaned 2-309 silicone elastomer O-rings at room temperature; (2) contamination with JSC-1A lunar regolith simulant severely impacted the leak rate values of 2-309 silicone elastomer O-rings at room temperature; (3) the leak rate values for contaminated 2-309 silicone elastomer O-rings at room temperature were immeasurably high using

the current system for all levels of compression excluding 100%; and (4) in general, removing the JSC-1A simulant via a mechanical brushing method returned the leak rate values measured at room temperature to as-received levels.

ACKNOWLEDGEMENTS

The authors acknowledge the contributions and technical support of Nicholas G. Garafolo and Janice L. Wasowski. This material is based upon work supported by the National Aeronautics and Space Administration under Contract Number NNC08CA35C.

REFERENCES

ASTM International (2003), ASTM E595-07 (reapproved 2003): Standard test method for total mass loss and collected volatile condensable materials from outgassing in a vacuum environment.

Bastrzyk, M. B. & Daniels, C. C. (2010), "The mechanical performance of subscale candidate elastomer docking seal", *in* 'Proceedings of the 51st AIAA Materials Conference', number AIAA 2010-3129, AIAA, Orlando, FL.

Carrell, T. R. & Blair, H. (1964), "Elastomeric seals in hard vacuum", *Journal of Spacecraft* **1**(1), 113–115.

Daniels, C. C. & Garafolo, N. G. (2010), "Comprehensive mass point leak rate technique. Part II: Application of methodology and variable influences", *in* 'JSNDI/ASNT Fourth Japan - US Symposium on Emerging NDE Capabilities for a Safer World', Maui, Hawaii.

Finkbeiner, J. R., Dunlap, Jr., P. H., Steinetz, B. M. & Daniels, C. C. (2008), "Review of seal designs on the Apollo spacecraft", *Journal of Spacecraft and Rockets* **45**(5), 900–910.

Gaier, J. R. (2005), "The effects of lunar dust on eva systems during the Apollo missions", Technical Report NASA/TM-2005-213610/REV1, NASA.

Garafolo, N. G. (2010), "A Compressible Advection Approach in Permeation of Elastomer Space Seals", Ph.D. Dissertation, The University of Akron.

Garafolo, N. G., Bastrzyk, M. B. & Daniels, C. C. (2010), "The effects of atomic oxygen on the sealing and mechanical performance of an elastomer seal", *in* 'Proceedings of the 48th AIAA Aerospace Sciences Meeting', number AIAA 2010-1440.

Garafolo, N. G. & Daniels, C. C. (2010), "Comprehensive mass point leak rate technique. Part I: Methodology with uncertainty and experimental error analysis", *in* 'JSNDI/ASNT Fourth Japan - US Symposium on Emerging NDE Capabilities for a Safer World', Maui, Hawaii.

Garafolo, N. G. & Daniels, C. C. (2011), "Contamination simulation of elastomer space seals with foreign object debris", *in* 'Proceedings from the 3rd AIAA Atmospheric Space Environments Conference', number AIAA-2011-3674, Honolulu, HI.

Garafolo, N. G. & Daniels, C. C. (2014), "The mass point leak rate technique with uncertainty analysis", *Research in Nondestructive Evaluation* **25**(2), 125–149.

Moore, P. O., Jackson, Jr., C. N. & Sherlock, C. N., eds (1998), *Nondestructive Testing Handbook, Leak Testing*, Vol. 1, 3rd edn, American Society for Nondestructive Testing, Inc.

National Aeronautics and Space Administration (1995), "Orbital debris: A technical assessment", Technical Report NASA-CR-198639, NASA.

National Aeronautics and Space Administration (2013), "Space debris and human spacecraft", http://www.nasa.gov/mission_pages/station/news/orbital_debris.html (Sept 27, 2013).

National Aeronautics and Space Administration (2007), NASA-STD-(I)-6016: Standard materials and processes requirements for spacecraft, expires September 2007.

Oravec, H. A., Panickar, M. B., Wasowski, J. L. & Daniels, C. C. (2011), "Influence of elastomer compound and test temperature on the compression force of candidate space seals: A preliminary study", *in* 'Proceedings of the 47th AIAA / ASME / SAE / ASEE Joint Propulsion Conference & Exhibit', number AIAA 2011-5709, AIAA, San Diego, CA.

Parker Hannifin Corporation (2001), *Parker O-Ring Handbook*, Parker Hannifin Corporation, Cleveland, Ohio.

Zeng, X., He, C., Oravec, H., Wilkinson, A., Agui, J. & Asnani, V. (2010), "Geotechnical properties of JSC-1A lunar soil simulant", *Journal of Aerospace Engineering* **23**(2), 111–116.